COMBINING PLASMACHEMICAL EMULSION-TEMPLATING WITH ATRP TO CREATE MACROPOROUS LIPOPHILIC SURFACES

P. S. Brown, T. J. Wood, and J. P. S. Badyal*

Department of Chemistry
Science Laboratories
Durham University
Durham DH1 3LE
England, UK

* Corresponding author email: j.p.badyal@durham.ac.uk

GRAPHICAL ABSTRACT

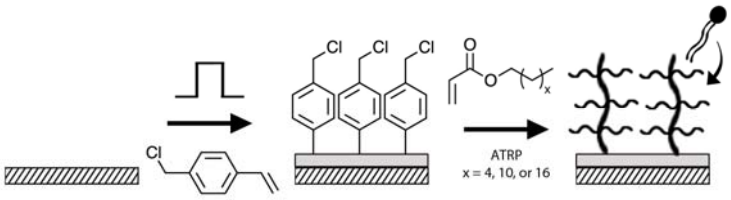

ABSTRACT

Well-defined alkyl chain side group polymer brushes have been tethered onto high surface area macroporous pulsed plasmachemical emulsion-templated poly(vinylbenzyl chloride) initiator layers (typically 600—700 m^2g^{-1}) using atom transfer radical polymerisation (ATRP). Immobilisation of phospholipids onto these bioactive surfaces is found to occur through interdigitation, and the efficacy of lipid binding is governed by the alkyl side group chain length of the polymer brushes.

Keywords: Functional surface; polymer brush; bioactive; phospholipids; emulsion-templating.

1. INTRODUCTION

Lipid biomolecules play a number of key roles in living systems.[1] For instance, phospholipids, which are a type of amphiphilic lipid comprising a hydrophilic phosphate head group and a straight chain hydrophobic tail group, provide an important structural role in the cell membrane (they form a lipid bilayer through hydrophobic interactions between tail groups).[2] Of particular interest is the immobilisation of phospholipids onto surfaces for the biofuntionalisation of substrates[3] for application in sensors,[4,5] diagnostics,[6] biomimetics,[7] biocompatibilty,[8] and separation science.[9] The most common approach employed for the surface immobilisation of phospholipids entails the formation of a surface-supported lipid bilayer.[10] These are typically prepared using surface-bound alkylsilane,[11,12] alkanethiol,[7,13,14,15] or thiolipid[10,16] self-assembled monolayers (SAMs). The inherent well-packed nature of such SAMs enables the formation of a *non-interdigitated* hybrid lipid bilayer comprising a layer of phospholipids on top of a layer of surface bound SAM alkyl chain molecules.[14,17] However, several inherent drawbacks limit their more widespread use, which include moisture sensitivity of silanes,[18,19,20] the instability of thiols towards oxidation,[21] the requirement for specific substrate surfaces for self-assembly (such as silicon,[22] glass,[23] gold,[24] platinum,[25] or palladium[26]), and the lack of readily available high surface area 3-dimensional variants.

In this article, a substrate-independent approach for the creation of lipophilic surfaces is reported. This entails the growth of alkyl acrylate polymer brushes by atom transfer radical polymerisation (ATRP)[27] from pulsed plasma deposited poly(vinylbenzyl chloride) initiator layers.[28] Pulsed plasma deposited polymer films can be tailored to a high degree of molecular specificity, where the short plasma duty cycle on-period (microseconds) generates active sites in the gas phase and at the growing film surface and these initiate conventional polymerisation reaction pathways during the longer plasma off- period (milliseconds).[29] Key advantages of pulsed plasmachemical deposition include substrate-independence (metal, inorganic, or polymer substrates) and easily scalable (e.g. roll-to-roll). In the present study, the degree of lipid binding to different alkyl chain length side group ATRP polymer brushes grown off pulsed plasma deposited poly(vinylbenzyl chloride) initiator layers is investigated by using a biotin-conjugated phospholipid, which is

then further tested for bioactivity by measuring the extent of binding to a fluorescently labelled avidin–FITC conjugate, Scheme 1. Furthermore, emulsion-templating is utilised to induce pore formation in the pulsed plasma deposited poly(vinylbenzyl chloride) initiator layers to create high surface area macroporous lipophilic surfaces (typically 600—700 m^2g^{-1}).

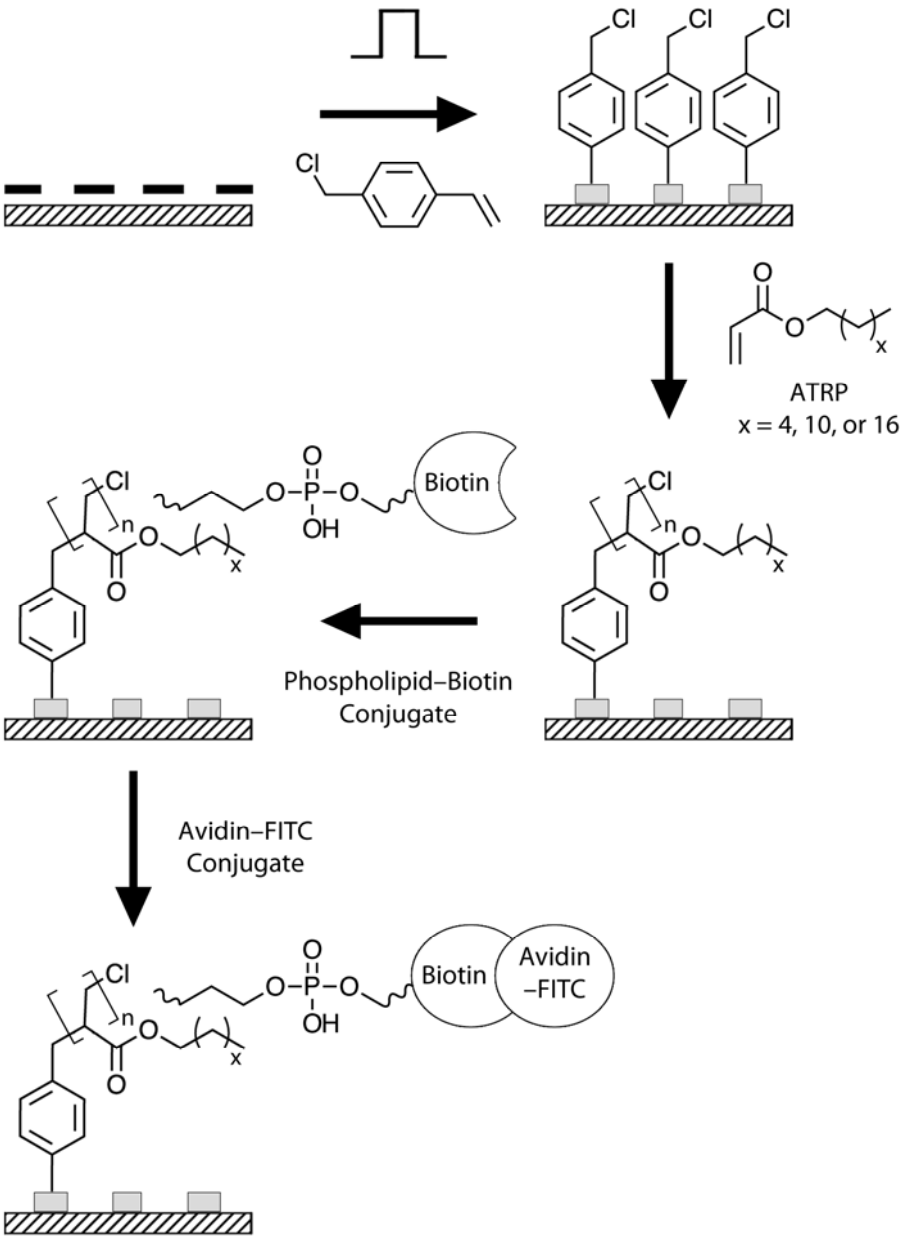

Scheme 1: Pulsed plasma deposition of poly(vinylbenzyl chloride) ATRP initiator layer through a mask followed by ATRP growth of alkyl acrylate polymer brushes (where *n* is the degree of polymerisation) to create patterned lipophilic surfaces. Demonstration of bioactivity by subsequent surface immobilisation of phospholipid–biotin conjugate, followed by binding to fluorescent avidin–FITC conjugate.

2. EXPERIMENTAL

2.1 Sample Preparation

Polished silicon (100) wafers (Silicon Valley Microelectronics, Inc.) and PTFE sheet (Goodfellow Cambridge Ltd.) were used as substrates. Vinylbenzyl chloride monomer (97%, mixture of 3- and 4- isomers, Sigma Aldrich Ltd.) was loaded into a sealable glass tube and further purified using multiple freeze-pump-thaw cycles. Pulsed plasmachemical deposition of the poly(vinylbenzyl chloride) initiator layer was carried out in a cylindrical glass chamber (5 cm diameter, 470 cm^3 volume) connected to a rotary pump via a liquid nitrogen cold trap (4 x 10^{-3} mbar base pressure and a leak rate better than 6 x 10^{-9} mol s^{-1}). An L-C matching unit was used to minimise the standing wave ratio between a 13.56 MHz power supply and a copper coil externally wound around the glass reactor. Prior to each plasma deposition, the chamber was scrubbed with detergent, rinsed in propan-2-ol, and further cleaned using a 50 W air plasma for 30 min. Next, the substrate to be coated was placed into the center of the reactor, and the system pumped down to base pressure. Vinylbenzyl chloride precursor vapor was introduced into the chamber at a pressure of 0.2 mbar for 5 min followed by ignition of the electrical discharge. The optimum duty cycle for structural retention of the benzyl chloride functionality corresponded to on-period = 100 μs and off-period = 4 ms in combination with peak power = 30 W.[28] Upon completion of deposition, the precursor vapour was allowed to continue to flow through the system for a further 5 min in order to quench any trapped reactive sites present within the deposited film. Patterned ATRP initiator layers were fabricated by depositing 100 nm thickness pulsed plasma poly(vinylbenzyl chloride) through a mask (brass mesh, 400 μm pore diameter). Preparation of plasmachemical emulsion-templated macroporous ATRP initiator samples entailed immersing substrates bearing 3 μm thick pulsed plasma deposited poly(vinylbenzyl chloride) layers into 0.15 mg L^{-1} aqueous solution of cresyl violet perchlorate (Sigma Aldrich Ltd.) for 16 h.[30] Following removal from solution, each sample was thoroughly rinsed with high purity water in order to remove excess cresyl violet perchlorate and soaked in fresh high purity water for an additional 16 h at room temperature (to leave cresyl violet perchlorate trapped within the pulsed plasma deposited poly(vinylbenzyl chloride) matrix). Each sample was then placed inside a sealed jar containing high purity water and stored at 60 °C for 1 h in order to induce

pore formation via emulsion templating (creation of pockets of hydrated cresyl violet perchlorate). Finally, this macroporous poly(vinylbenzyl chloride) ATRP initiator layer was dried under ambient conditions for 16 h.

For surface atom transfer radical polymerisation (ATRP), each pulsed plasma poly(vinylbenzyl chloride) initiator layer coated substrate was loaded into a sealable glass tube containing copper(I) bromide (5 mmol, 98%, Sigma Aldrich Ltd.), 2-2'-bipyridyl (10 mmol, +98%, Sigma Aldrich Ltd.), toluene (10 mL, Fisher Scientific UK Ltd.), and the appropriate alkyl acrylate monomer (either hexyl acrylate (0.05 mol, 98%, Sigma Aldrich Ltd.), dodecyl acrylate (0.05 mol, 90%, Sigma Aldrich Ltd.), or octadecyl acrylate (0.05 mol, 97%, Sigma Aldrich Ltd.)). The mixture was thoroughly degassed using several freeze-pump-thaw cycles and then immersed into an oil bath maintained at 95 ºC for 5 h to allow surface ATRP polymer brush growth, Scheme 1. Finally, cleaning and removal of any physisorbed polymer was undertaken by Soxhlet extraction with hot toluene for 16 h. In the case of the macroporous poly(vinylbenzyl chloride) ATRP initiator layer, the water trapped within the pores during emulsion-templating is displaced by the solvents used during ATRP to give typical surface areas of 600—700 m^2g^{-1}).[31]

2.2 Lipid Binding

In order to demonstrate bioactivity, ATRP alkyl polymer brush surfaces were immersed for 10 min into a phosphate buffered saline solution containing 20 μg mL^{-1} phospholipid–biotin conjugate (KODE Biotech Ltd) followed by extensive rinsing with high purity water, and then washing in phosphate buffered saline for 16 h, Scheme 1. These surfaces were subsequently immersed for 10 min into a second phosphate buffered saline solution containing 20 μg mL^{-1} fluorescent avidin–FITC conjugate (Invitrogen Corp.), followed by repeat rinsing with high purity water, and finally washing in phosphate buffered saline for 16 h.

2.3 Surface Characterisation

A VG ESCALAB spectrometer equipped with an unmonochromatised Mg K_α X-ray source (1253.6 eV) and a concentric hemispherical analyser (CAE mode pass energy = 20 eV) was used for X-ray photoelectron spectroscopy (XPS) analysis. The C(1s) XPS spectra were referenced to the (-$\underline{C}_xH_y$) hydrocarbon peak at 285.0 eV,

and fitted to a linear background and equal full-width-at-half maximum (FWHM) Gaussian components.[32] Elemental compositions were calculated using sensitivity (multiplication) factors derived from chemical standards, C(1s): O(1s): Cl(2p) = 1.00: 0.34: 0.37.

Fourier transform infrared (FTIR) analysis of the deposited layers was undertaken using a Perkin-Elmer Spectrum One FTIR instrument equipped with a liquid nitrogen cooled MCT detector. Spectra were recorded at a resolution of 4 cm^{-1} across the 700–4000 cm^{-1} wavelength range. Reflection absorption infrared spectroscopy (RAIRS) measurements were performed using a variable angle accessory (Specac Ltd.) set at 66° and fitted with a KRS-5 polarizer to remove the s-polarized component.

Thickness measurements of films deposited onto silicon wafers were made using a spectrophotometer (nkd-6000, Aquila Instruments Ltd). The obtained transmittance-reflectance curves (350–1000 nm wavelength range) were fitted to a Cauchy model for dielectric materials using a modified Levenberg-Marquardt method.[33]

Microlitre sessile drop contact angle analysis was carried out with a video capture system (VCA2500XE, AST Products Inc.) using 1.0 µL dispensation of de-ionised water. Contact angle values were taken after 10 s, and carried out in 5 different locations on at least 3 separate samples.

Fluorescence microscopy was performed using an Olympus IX-70 system (DeltaVision RT, Applied Precision Inc.). Images were collected on at least 3 separate samples.using excitation wavelengths at 490±25 nm and emission wavelengths at 528±40 nm (which corresponds to the absorption/emission maxima of 494/518 nm for the FITC fluorescent tag).

3. RESULTS AND DISCUSSION

XPS analysis of the pulsed plasma deposited poly(vinylbenzyl chloride) ATRP initiator layer confirmed complete coverage of the silicon substrate with no underlying Si(2p) signal detected. In addition, the measured elemental compositions are in good agreement with calculated theoretical values based on the vinylbenzyl chloride precursor, Table 1, thereby suggesting good structural retention of the benzyl chloride functionality. This was confirmed by infrared spectroscopy, where the main fingerprint absorbances match those associated with the monomer;[28] these include CH_2-Cl wag (1263 cm^{-1}) and benzyl stretches (1495 and 1603 cm^{-1}), Figure 1. Furthermore, the disappearance of the vinyl double bond (1629 cm^{-1}) is consistent with polymerization taking place.

Table 1: XPS elemental compositions and static water contact angles of: pulsed plasma deposited poly(vinylbenzyl chloride) initiator layer; surface ATRP poly(hexyl acrylate) brushes; surface ATRP poly(dodecyl acrylate) brushes; and surface ATRP poly(octadecyl acrylate) brushes. Where the calculated theoretical elemental composition values are based on an ideal polymer repeat unit derived from the monomer structure, and include an end capping chlorine atom associated with the ATRP polymerization mechanism. [34]

Layer	XPS Elemental Composition / ±0.5%			Static Water Contact Angle / ±1°
	% C	% Cl	% O	
Pulsed Plasma poly(vinylbenzyl chloride)	86.8	9.6	3.6	80
Theoretical poly(vinylbenzyl chloride)	90.0	10.0	0.0	-
ATRP hexyl acrylate	76.2	7.7	16.1	69
Theoretical ATRP hexyl acrylate	75.0	8.3	16.7	-
ATRP dodecyl acrylate	84.0	5.3	10.7	72
Theoretical ATRP dodecyl acrylate	83.3	5.6	11.1	-
ATRP octadecyl acrylate	86.4	5.2	8.3	78
Theoretical ATRP octadecyl acrylate	87.5	4.2	8.3	-

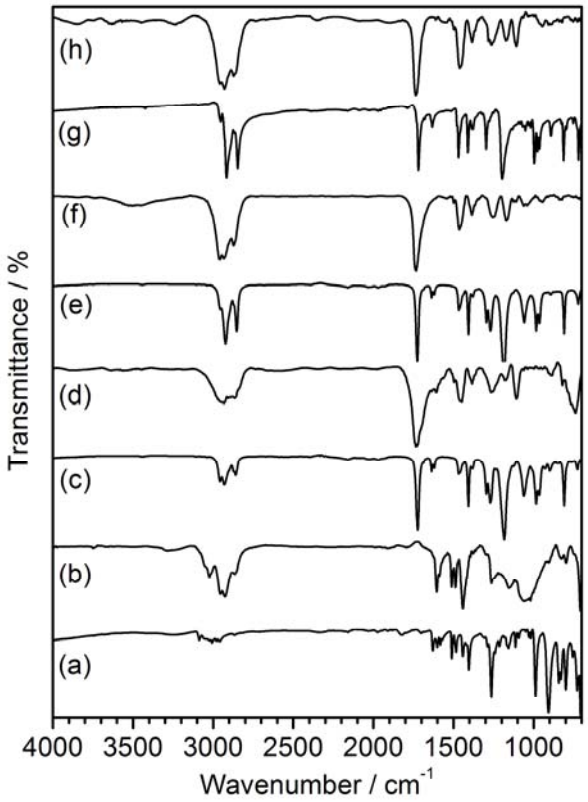

Figure 1: Infrared spectra of: (a) vinylbenzyl chloride monomer; (b) pulsed plasma deposited poly(vinylbenzyl chloride) ATRP initiator layer; (c) hexyl acrylate monomer; (d) ATRP poly(hexyl acrylate) brushes; (e) dodecyl acrylate monomer; (f) ATRP poly(dodecyl acrylate) brushes; (g) octadecyl acrylate monomer; and (h) ATRP poly(octadecyl acrylate) brushes.

Atom transfer radical polymerisation (ATRP) of the alkyl acrylate monomers onto the pulsed plasma deposited poly(vinylbenzyl chloride) initiator layers was confirmed by XPS, water contact angle, and FTIR analysis, Table 1 and Figure 1. The measured XPS elemental compositions are consistent with surface grafted alkyl acrylate polymers with an end capping chlorine (indicative of the ATRP mechanism[34]). Water contact angle value increases with polymer brush alkyl side group chain length which correlates to greater hydrophobicity. Infrared assignments for hexyl acrylate monomer and its corresponding surface tethered ATRP polymer brushes are as follows:[35] terminal methyl group C-H stretching (2957 cm^{-1}), anti-symmetric CH stretching (2931 cm^{-1}), symmetric C-H stretching (2860 cm^{-1}), C=O stretching (1724 cm^{-1}), and C=C stretching (1637 cm^{-1}). For the case of dodecyl acrylate monomer and its surface grafted ATRP polymer brushes: terminal methyl group C-H stretching (2957 cm^{-1}), anti-symmetric CH stretching (2921 cm^{-1}), symmetric C-H stretching (2854 cm^{-1}), C=O stretching (1726 cm^{-1}), and C=C

stretching (1637 cm^{-1}). Whilst for the octadecyl acrylate monomer and its surface grafted ATRP polymer brushes: terminal methyl group C-H stretching (2952 cm^{-1}), anti-symmetric CH stretching (2915 cm^{-1}), symmetric C-H stretching (2846 cm^{-1}), C=O stretching (1733 cm^{-1}), C=C stretching (1632 cm^{-1}), and C-CH_3 bending (1366 cm^{-1}). For all of the ATRP polymer brush layers, polymerisation at the acrylate centre was confirmed by the absence of the C=C stretching (1632 cm^{-1}) absorbance.

In order to demonstrate bioactivity, these alkyl polymer brush functionalised surfaces were washed sequentially in solutions containing phospholipid–biotin conjugate and then avidin–FITC conjugate leading to binding of the fluorescently labelled avidin to the biotin of the phospholipid[36], Scheme 1. The efficacy of phospholipid surface binding was quantified by measuring the signal intensity of the FITC fluorescent tag[37], Figure 2. It was found that the degree of phospholipid binding is dependent upon the alkyl chain length of the alkyl acrylate monomer employed during surface ATRP, Figure 2. The fluorescence intensity correlates linearly to alkyl chain length, which is consistent with phospholipid binding being dependent upon a hydrophobic interaction.[38,39,40,41] By increasing the chain length of the alkyl acrylate monomer used during the ATRP reaction, the hydrophobic interaction between the alkyl side groups and the phospholipid increases, and the lipid binds more strongly to the polymer brush, which makes it more resilient towards subsequent washing steps, thereby yielding a more intense fluorescence signal. This dependence upon alkyl chain length suggests that the lipid tail interacts with the polymer alkyl side chain directly (interdigitation) *in lieu* of forming a hybrid bilayer (as reported for previous SAM studies where the chain length is considered to have little effect on the strength of the SAM–lipid interaction[14] or the formation of a bilayer[42]).

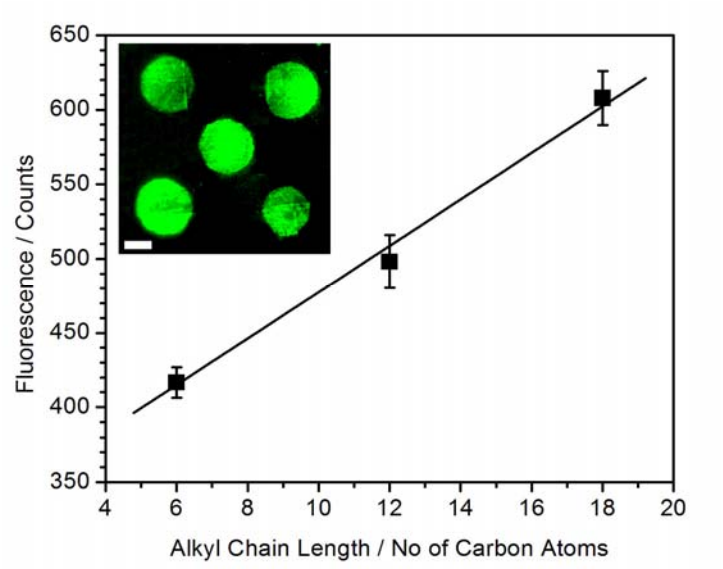

Figure 2: Fluorescence signal following exposure to phospholipid–biotin conjugate, and then binding with fluorescent avidin–FITC conjugate, as a function of alkyl side group chain length of surface tethered ATRP polymer brushes (20 nm thickness) grown off pulsed plasma deposited poly(vinylbenzyl chloride) initiator layer (100 nm thickness). Inset: Corresponding fluorescence image of a patterned lipophilic surface comprising ATRP poly(octadecyl acrylate) brushes grown from pulsed plasma deposited poly(vinylbenzyl chloride), scale bar = 200 μm.

By altering the ATRP reaction period, it is possible to vary the length of the surface grafted polymer brushes. However, it was found that the length of the polymer brush has little effect on the measured fluorescence intensity, thereby confirming that phospholipid immobilisation occurs primarily via hydrophobic interaction with the surface polymer brush alkyl side groups. Furthermore, control experiments showed that low fluorescence signal intensity was measured following exposure of the more hydrophobic pulsed plasma deposited poly(vinylbenzyl chloride) ATRP initiator layers to the phospholipid–biotin and avidin–FITC conjugate solutions, thereby confirming that the surface tethered alkyl chain polymer brushes (i.e. interdigitation) are necessary for phospholipid immobilisation to occur (rather than greater hydrophobicity), Table 1.

Formation of an emulsion-templated macroporous (poly(HIPE)) pulsed plasma deposited poly(vinylbenzyl chloride) initiator layer entailed immersion in aqueous cresyl violet solution followed by washing and heating in water at 60 °C for 1 h in order to induce pore formation (creation of pockets of hydrated cresyl violet perchlorate within the poly(vinylbenzyl chloride) initiator layer) and provide typically 600–700 m^2 g^{-1} surface area.[30,31] Infrared analysis supports this with the porous

poly(vinylbenzyl chloride) retaining the benzyl chloride functionality (1263 cm^{-1}), and a broad H-O-H bend absorbance at 1690 cm^{-1} attributed to water associated with cresyl violet perchlorate during pore formation[30], Figure 3. Surface ATRP growth of alkyl acrylate polymer brushes off this pulsed plasma deposited emulsion-templated macroporous poly(vinylbenzyl chloride) initiator layer led to the appearance of the characteristic poly(alkyl acrylate) C=O stretch (1733 cm^{-1}). Phospholipid–biotin attachment onto these surfaces through interdigitation and subsequent avidin–FITC conjugate binding with was confirmed by fluorescence microscopy, Figure 4. No phospholipid–biotin tethering to the macroporous poly(vinylbenzyl chloride) initiator layer was observed in the absence of the surface grafted ATRP poly(alkyl acrylate) brushes.

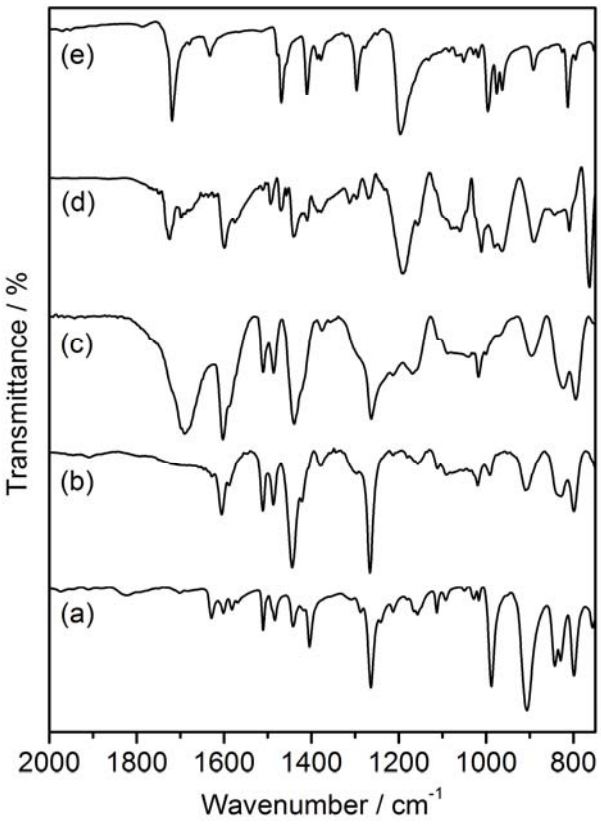

Figure 3: Infrared spectra of: (a) vinylbenzyl chloride monomer; (b) pulsed plasma deposited poly(vinylbenzyl chloride); (c) pulsed plasma deposited emulsion-templated macroporous poly(vinylbenzyl chloride) initiator layer; (d) ATRP poly(dodecyl acrylate) brushes grown from (c); and (e) dodecyl acrylate monomer.

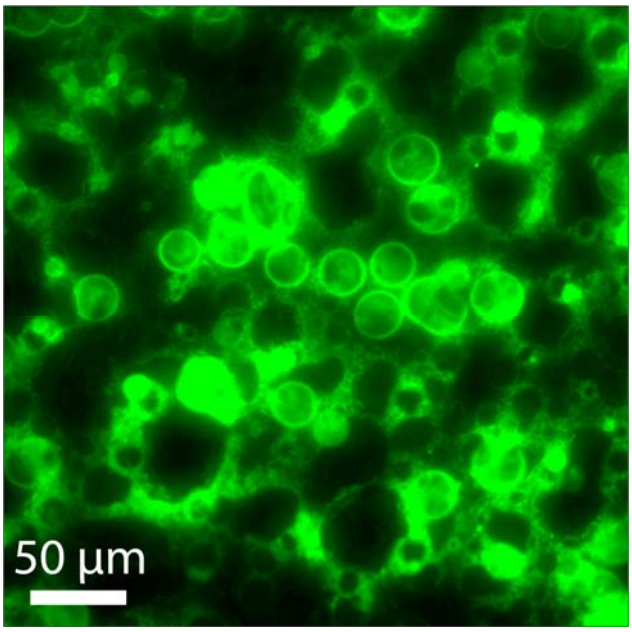

Figure 4: Fluorescence image of ATRP poly(octadecyl acrylate) brushes grown from plasmachemical emulsion-templated macroporous poly(vinylbenzyl chloride) initiator layer, following exposure to phospholipid–biotin conjugate, and then binding with fluorescent avidin–FITC conjugate.

4. CONCLUSIONS

Lipophilic, macroporous bioactive surfaces have been fabricated using ATRP alkyl side group polymer brushes grown off plasmachemical emulsion-templated poly(vinylbenzyl chloride) initiator layers. The degree of phospholipid binding is found to increase in a linear fashion with respect to the alkyl side group chain length of the surface tethered ATRP polymer brushes, and is taken to be indicative of the lipid tails interacting with the polymer alkyl side chains through interdigitation. These lipophilic surfaces are of potential interest for 3-D tissue engineering scaffolds, as well as biosensors and bioarrays. The inherent substrate-independence (including flexible substrates) and high surface areas (typically 600–700 m^2 g^{-1}) offer distinct advantages compared to conventional self-assembled monolayer (SAM) techniques.

5. ACKNOWLEDGEMENTS

We are grateful to KODE Biotech Ltd (New Zealand) for providing a sample of the phospholipid–biotin conjugate.

6. REFERENCES

[1] Brown, H. A.; Marnett, L. J. *Chem. Rev.* **2011**, *111*, 5817.

[2] Brown, H. A.; Murphy, R. C. *Nat. Chem. Biol.* **2009**, *5*, 602.

[3] Sackmann, E. *Science* **1996**, *271*, 43.

[4] Cornell, B. A.; Braach-Maksvytis, V. L. B.; King, L. G.; Osman, P. D. J.; Raguse, B.; Wieczorek, L.; Pace, R. J. *Nature* **1997**, *387*, 580.

[5] Stora, T.; Lakey, J. M.; Vogel, H. *Angew. Chemie. Int. Ed.* **1999**, *38*, 389.

[6] Moran-Mirabel, J. M.; Edel, J. B.; Meyer, G. D.; Throckmorton, D.; Singh, A. K.; Craighead, H. G. *Biophys. J.* **2005**, *89*, 296.

[7] Plant, A. L.; Gueguechkeri, M.; Yap, W. *Biophys. J.* **1994**, *67*, 1126.

[8] Mornet, S.; Lambert, O.; Duguet, E.; Brisson, A. *Nano Lett.* **2005**, *5*, 281.

[9] van Oudenaarden, A.; Boxer, S. G. *Science* **1999**, *285*, 1046.

[10] Lang, H.; Duschl, C.; Gratzel, M.; Vogel, H. *Thin Solid Films* **1992**, *210–211*, 818.

[11] Wagner, M. L.; Tamm, L. K. *Biophys. J.* **2000**, *79*, 1400.

[12] Atanasov, V.; Knorr, N.; Duran, R. S.; Ingebrandt, S.; Offenhäusser, A.; Knoll, W.; Köper, I. *Biophys. J.* **2005**, *89*, 1780.

[13] Edinger, K.; Goelzhaeuser, A.; Demota, K.; Woell, C.; Grunze, M. *Langmuir* **1993**, *9*, 4.

[14] Meuse, C. W.; Niaura, G.; Lewis, M. L.; Plant, A. L. *Langmuir*, **1998**, *14*, 1604.

[15] Terrettaz, S.; Stora, T.; Duschl, C.; Vogel, H. *Langmuir* **1993**, *9*, 1361.

[16] Lingler, S.; Rubinstein, I.; Knoll, W.; Offenhäusser, A. *Langmuir* **1997**, *13*, 7085.

[17] Hubbard, J. B.; Silin, V.; Plant, A. L. *Biophys. Chem.* **1998**, *75*, 163.

[18] Ulman, A. *Chem. Rev.*, **1996**, *96*, 1533.

[19] Wang, M.; Liechti, K. M.; Wang, Q.; White, J. M. *Langmuir* **2005**, *21*, 1848.

[20] Hancer, *Prog. Org. Coat.*, 2008, **63**, 395.

[21] Lee, M.-T.; Hsueh, C.-C.; Freund, M. S.; Ferguson, G. S. *Langmuir* **1998**, *14*, 6419.

[22] Linford, M. R.; Chidsey, C. E. D.; *J. Am. Chem. Soc.* **1993**, *115*, 12631.

[23] Sagiv, J. *J. Am. Chem. Soc.* **1980**, *102*, 92.

[24] Bain, C. D.; Troughton, E. B.; Tao, Y. T.; Evall, J.; Whitesides, G. M.; Nuzzo, R. G. *J. Am. Chem. Soc.* **1989**, *111*, 321.

[25] Tu, W.; Takai, K.; Fukui, K.-I.; Miyazaki, A.; Enoki, T. *J. Phys. Chem. B* **2003**, *107*, 10134.

[26] Stapleton, J. J.; Daniel, T. A.; Uppili, S.; Cabarcos, O. M.; Naciri, J.; Shashidhar, R.; Allara, D. L. *Langmuir* **2005**, *21*, 11061.

[27] Wang, J.-S.; Matyjaszewski, K. *J. Am. Chem. Soc.* **1995**, *117*, 5614.

[28] Teare, D. O. H.; Barwick, D. C.; Schofield, W. C. E.; Garrod, R. P.; Ward, L. J.; Badyal, J. P. S. *Langmuir* **2005**, *21*, 11425.

[29] Ryan, M. E.; Hynes, A. M.; Badyal, J. P. S. *Chem. Mater.* **1996**, *8*, 37.

[30] Morsch, S.; Wood, T. J.; Schofield, W. C. E.; Badyal, J. P. S. *Adv. Funct. Mater.* **2012**, *22*, 313.

[31] Schofield, W. C. E.; Bain, C. D.; Badyal, J. P. S. *Chem. Mater.* **2012**, *24*, 1645.

[32] Evans, J. F.; Gibson, J. H.; Moulder, J. F.; Hammond, J. S.; Goretzki, H. *Fresenius J. Anal. Chem*. **1984**, *841*, 319.

[33] Tabet, M. F.; McGahan, W. A. *Thin Solid Films* **2000**, *370*, 122.

[34] Zhang, H.; Schubert, U. S. *J. Polym. Sci., Part A: Polym. Chem.* **2004**, *42*, 4882.

[35] Lin-Vien, D.; Colthup, N. B.; Fateley; W. G.; Grasselli, J. G. *The Handbook of Infrared and Raman Characteristic Frequencies of Organic Molecules*, Academic Press, London, 1991.

[36] Snell, E. E.; Eakin, R. E.; Williams, R. J. *J. Am. Chem Soc.* **1940**, *62*, 175.

[37] Zhao, S.; Reichert, W. M. *Langmuir* **1992**, *8*, 2785.

[38] Su, J. Y.; Hodges, R. S.; Kay, C. M. *Biochemistry* **1994**, *33*, 15501.

[39] Okuzaki, H.; Osada, Y. *Macromolecules* **1994**, *27*, 502.

[40] Borden, M. A.; Longo, M. L. *Langmuir* **2002**, *18*, 9225.

[41] Kim, D. H.; Costello, M. J.; Duncan, P. B.; Needham, D. *Langmuir* **2003**, *19*, 8455.

[42] Plant, A. L. *Langmuir* **1993**, *9*, 2764.